

THE PROXIMAL MAP OF THE WEIGHTED MEAN ABSOLUTE ERROR*

Lukas Baumgärtner[†] Roland Herzog[‡] Stephan Schmidt[†] Manuel Weiß[‡]

We investigate the proximal map for the weighted mean absolute error function. An algorithm for its efficient and vectorized evaluation is presented. As a demonstration, this algorithm is applied as part of a checkerboard algorithm to solve a total-variation image denoising (ROF) problem as well as a non-smooth energy minimization problem.

Keywords. proximal map, weighted mean absolute error, multi-thresholding

AMS subject classifications (MSC2010). 90C25, 68U10, 94A08, 46N10

1 INTRODUCTION

The proximity operator, or proximal map, plays a fundamental role in non-smooth optimization; see for instance [Chambolle, Pock, 2011](#); [Combettes, Pesquet, 2011](#); [Parikh, Boyd, 2014](#). Given a function $f: \mathbb{R}^n \rightarrow \mathbb{R} \cup \{\infty\}$, the proximal map $\text{prox}_f: \mathbb{R}^n \rightarrow \mathbb{R}^n$ is defined as the solution of the problem

$$\text{Minimize } f(y) + \frac{1}{2} \|y - x\|_2^2, \quad \text{where } y \in \mathbb{R}^n. \quad (1.1)$$

Under the mild condition that f is proper, lower semicontinuous and convex, prox_f is well-defined. We refer the reader to [Bauschke, Combettes, 2011](#), Ch. 12.4 for details and further properties.

In this paper we present theory and an efficient algorithm for the evaluation of prox_f , where $f: \mathbb{R} \rightarrow \mathbb{R}$ is defined as

$$f(x) := \sum_{i=1}^N w_i |x - d_i|. \quad (1.2)$$

*This work was supported by DFG grants HE 6077/10-2 and SCHM 3248/2-2 within the Priority Program SPP 1962 (Non-smooth and Complementarity-based Distributed Parameter Systems: Simulation and Hierarchical Optimization), which is gratefully acknowledged.

[†]Institut für Mathematik, Humboldt-Universität zu Berlin, 10099 Berlin, Germany (lukas.baumgaertner@hu-berlin.de, <https://www.mathematik.hu-berlin.de/en/people/mem-vz/1693318>, ORCID 0000-0003-1007-4815, s.schmidt@hu-berlin.de, <https://www.mathematik.hu-berlin.de/en/people/mem-vz/1693090>, ORCID 0000-0002-4888-0794).

[‡]Interdisciplinary Center for Scientific Computing, Heidelberg University, 69120 Heidelberg, Germany (roland.herzog@iwr.uni-heidelberg.de, <https://scoop.iwr.uni-heidelberg.de>, ORCID 0000-0003-2164-6575, manuel.weiss@iwr.uni-heidelberg.de, <https://scoop.iwr.uni-heidelberg.de>, ORCID 0000-0002-6098-9725).

Here $w_i > 0$ are given, positive weights and $d_i \in \mathbb{R}$ are given data, $i = 1, \dots, N$ for some $N \in \mathbb{N}$. We refer to (1.2) as the weighted mean absolute error. Any of its minimizers is known as a weighted median of the data $\{d_i\}$. Clearly, f is proper, continuous and convex, and so is γf for any $\gamma > 0$.

By definition, the proximal map $\text{prox}_{\gamma f}: \mathbb{R} \rightarrow \mathbb{R}$ for f as in (1.2) is given by

$$\text{prox}_{\gamma f}(x) := \arg \min_{y \in \mathbb{R}} \gamma \sum_{i=1}^N w_i |y - d_i| + \frac{1}{2}(y - x)^2. \quad (1.3)$$

In the case of a single data point ($N = 1$), problem (1.3) reduces to the well-known problem

$$\arg \min_{y \in \mathbb{R}} \gamma w |y - d| + \frac{1}{2}(y - x)^2 \quad (1.4)$$

with $w > 0$ and $d \in \mathbb{R}$, whose unique solution is explicitly given in terms of the soft-thresholding operator $S_r(x) := \max\{0, |x| - r\} \text{sgn}(x)$. In this case, we have

$$\text{prox}_{\gamma f}(x) = d + S_{\gamma w}(x - d) = d + \max\{0, |x - d| - \gamma w\} \text{sgn}(x - d). \quad (1.5)$$

This map, often with $d = 0$, arises in many iterative schemes for the solution of problems involving the 1-norm; see for instance [Daubechies, Defrise, De Mol, 2004](#); [Goldstein, Osher, 2009](#). We can therefore view (1.3) as a multi-thresholding operation.

We wish to point out that our problem of interest (1.3) is different from the LASSO problem

$$\text{Minimize } \|Ay - d\|_2^2 + \lambda \|y\|_1 \quad \text{where } y \in \mathbb{R}^n, \quad (1.6)$$

see [Tibshirani, 1996](#); [Chen, Donoho, Saunders, 1998](#). In the latter, y is multi-dimensional and the deviation of its image under a linear map A from a data vector d is measured. By contrast, in (1.3) we measure the deviation of a scalar y from multiple data points d_i . Moreover, the roles of the 1-norm and the 2-norm are reversed in (1.3) and (1.6).

We point out that [Li, Osher, 2009](#) have considered the slightly more general problem

$$\arg \min_{y \in \mathbb{R}} \sum_{i=1}^N w_i |y - d_i| + F(y) \quad (1.7)$$

with F strictly convex, differentiable and F' bijective. The prototypical examples are functions $F(y) = \lambda |y - x|^\alpha$ with $\alpha > 1$. We concentrate on the case $F(y) = \frac{1}{2\gamma}(y - x)^2$, which agrees with (1.3). In contrast to [Li, Osher, 2009](#), we provide a vectorized, open-source implementation of (1.3); see [Baumgärtner et al., 2023](#). We also demonstrate the utility of our implementation of (1.3) by solving, similarly as in [Li, Osher, 2009](#), an image denoising problem using a block coordinate descent (checkerboard) algorithm. In order to overcome the generic failure of convergence of such a method to the unique minimizer, we combine it with restarts based on the steepest descent direction. The emphasis in this paper, however, is on the efficient solution of (1.3).

This paper is structured as follows: We establish an algorithm for the evaluation of the proximal map of the weighted mean absolute error (1.3) in [Section 2](#) and prove its correctness in [Theorem 2.1](#). In [Section 3](#) we briefly discuss the structural properties of the proximal map. We conclude by showing two applications of the proposed algorithm. The first application is to an image denoising problem using the ROF model [Rudin, Osher, Fatemi, 1992](#), see [Section 4](#). In [Section 5](#), we address a non-smooth energy minimization problem.

2 ALGORITHM FOR THE EVALUATION OF THE PROXIMAL MAP

In this section, we derive an efficient algorithm for the evaluation of the proximal map $\text{prox}_{\gamma f}(x)$ (1.3) and prove its correctness in [Theorem 2.1](#). To this end, we assume that the points d_i have been sorted and duplicates have been removed and their weights added. As a result, we can assume $d_1 < d_2 < \dots < d_N$. Moreover, we assume $\gamma > 0$, $N \geq 1$ and $w_i > 0$ for all $i = 1, \dots, N$. Summands with $w_i = 0$ can obviously be dropped from the sum in (1.3).

We divide the real line into the intervals

$$I_1 := (-\infty, d_1], \quad I_i := [d_{i-1}, d_i] \text{ for } i = 2, \dots, N \quad \text{and} \quad I_{N+1} := [d_N, \infty), \quad (2.1)$$

which overlap in the given data points. It is also useful to set $d_0 := -\infty$ and $d_{N+1} := \infty$. We further introduce the forward and reverse cumulative weights as

$$\mu_i := \sum_{k=1}^i w_k, \quad \nu_i := \sum_{k=i}^N w_k, \quad i = 1, \dots, N. \quad (2.2)$$

We extend these definitions by setting $\mu_0 := 0$, $\mu_{N+1} := \mu_N$ and $\nu_{N+1} := \nu_{N+2} := 0$. We therefore have $\nu_i = \mu_N - \mu_{i-1}$ for all $i = 1, \dots, N+2$. Using this notation, we can rewrite the derivative of f as

$$f'(y) = \mu_{i-1} - \nu_i \quad \text{for } y \in \text{int } I_i = (d_{i-1}, d_i), \quad i = 1, \dots, N+1. \quad (2.3)$$

This formula reflects the fact that f is piecewise linear and convex since $\mu_{i-1} - \nu_i$ is monotone increasing with i . Moreover, $f'(y) = \mu_0 - \nu_1 = -\sum_{k=1}^N w_k < 0$ holds for all $y \in \text{int } I_1$ (points to the left of smallest data point d_1), and $f'(y) = \mu_N - \nu_{N+1} = \sum_{k=1}^N w_k > 0$ holds for all $y \in \text{int } I_{N+1}$ (points to the right of the largest data point d_N). At $y = d_i$, $i = 1, \dots, N$, f is non-differentiable but we can specify its subdifferential, which is

$$\partial f(d_i) = [\mu_{i-1} - \nu_i, \mu_i - \nu_{i+1}], \quad i = 1, \dots, N. \quad (2.4)$$

The objective

$$\Phi(y) := \gamma f(y) + \frac{1}{2}(y-x)^2 = \gamma \sum_{i=1}^N w_i |y - d_i| + \frac{1}{2}(y-x)^2 \quad (2.5)$$

of (1.3) is piecewise quadratic and strongly convex. Its derivative is thus strongly monotone and it satisfies

$$\Phi'(y) < 0 \quad \text{for all } y < \min\{d_1, x\} \quad \text{and} \quad \Phi'(y) > 0 \quad \text{for all } y > \max\{d_N, x\}. \quad (2.6)$$

Consequently, the unique minimizer of Φ lies between these bounds.

The idea to finding the unique minimizer y^* of (2.5) is to locate the smallest index $1 \leq k \leq N+1$ such that $y^* \leq d_k$ holds, i. e., the nearest data point to the right of y^* . In other words, we need to find $1 \leq k \leq N+1$ such that

$$\lim_{y \searrow d_{k-1}} \Phi'(y) = \gamma (\mu_{k-1} - \nu_k) + d_{k-1} - x < 0 \quad (2.7a)$$

$$\text{and} \quad \lim_{y \searrow d_k} \Phi'(y) = \gamma (\mu_k - \nu_{k+1}) + d_k - x \geq 0 \quad (2.7b)$$

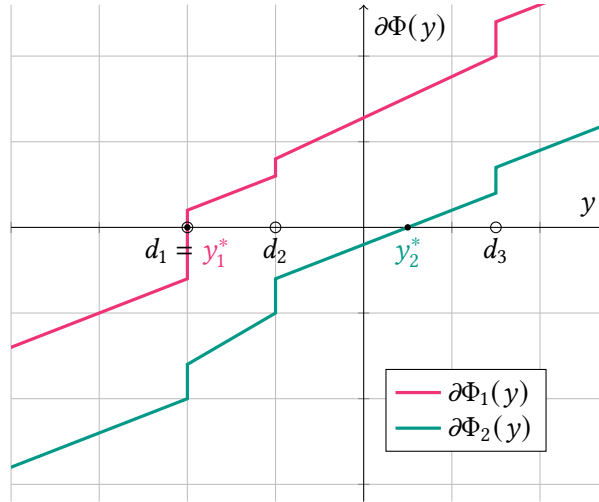


Figure 2.1: Visualization of the subdifferential $\partial\Phi$ of the objective Φ . In the first (upper) case, $y_1^* = d_1$ holds. In the second (lower) case, we have $y_2^* \in \text{int } I_3$.

holds. Now we can distinguish two cases: $y^* = d_k$ and $y^* < d_k$. The first case applies if and only if

$$\gamma(\mu_{k-1} - v_k) + d_k - x \leq 0. \quad (2.8)$$

Otherwise, y^* lies in $\text{int } I_k$ and thus it is the unique minimizer $x - \gamma(\mu_{k-1} - v_k)$ of the locally quadratic objective Φ . In either case, once the index $1 \leq k \leq N + 1$ has been identified, y^* is given by

$$y^* = \min\{d_k, x - \gamma(\mu_{k-1} - v_k)\}. \quad (2.9)$$

Both cases are also depicted in [Figure 2.1](#).

The considerations above lead to [Algorithm 1](#). In our implementation, we evaluate (2.10) for all k simultaneously and benefit from the quantities being monotone increasing with k when finding the first non-negative entry.

Algorithm 1 Evaluation of (1.3), the proximal map of the weighted mean absolute error.

Input: data points $d_1 < d_2 < \dots < d_N \in \mathbb{R}$, $N \geq 1$, and $d_0 := -\infty$, $d_{N+1} := \infty$

Input: weight vector $w \in \mathbb{R}^N$ with entries $w_i > 0$

Input: prox parameter $\gamma > 0$ and point of evaluation $x \in \mathbb{R}$

Output: $y = \text{prox}_{\gamma f}(x)$, the unique solution of (1.3)

- 1: Find the smallest index $1 \leq k \leq N + 1$ that satisfies

$$\gamma(\mu_k - v_{k+1}) + d_k - x \geq 0 \quad (2.10)$$

- 2: **return** $y := \min\{d_k, x - \gamma(\mu_{k-1} - v_k)\}$
-

Let us prove the correctness of [Algorithm 1](#).

Theorem 2.1. *Under the assumptions stated in [Algorithm 1](#), it returns $y^* = \text{prox}_{\gamma f}(x)$, the unique solution of (1.3).*

Proof. Let $1 \leq k \leq N + 1$ be the index found in [Line 1](#). First suppose $2 \leq k \leq N$. Then d_{k-1} and d_k are both finite, and (2.7), (2.10) imply

$$\max \partial\Phi(d_{k-1}) = \lim_{y \searrow d_{k-1}} \Phi'(y) < 0 \quad \text{and} \quad \max \partial\Phi(d_k) = \lim_{y \searrow d_k} \Phi'(y) \geq 0.$$

Owing to the properties of the subdifferential of strongly convex functions, there exists a unique point $y^* \in (d_{k-1}, d_k]$ such that $0 \in \partial\Phi(y^*)$, i. e., y^* is the unique minimizer of (1.3). This point either belongs to $\text{int } I_k$, or else $y^* = d_k$ holds. In the first case, Φ is differentiable, so that $\Phi'(y^*) = 0$ holds, yielding

$$x - \gamma(\mu_{k-1} - \nu_k) = y^* < d_k.$$

Otherwise, we have $y^* = d_k$, and $0 \in \partial\Phi(d_k)$ implies

$$d_k \leq x - \gamma(\mu_{k-1} - \nu_k). \quad (2.11)$$

In either case, the unique solution y^* of (1.3) is determined by

$$y^* = \min\{d_k, x - \gamma(\mu_{k-1} - \nu_k)\},$$

which is the quantity returned in [Line 2](#).

It remains to verify the marginal cases $k = 1$ and $k = N + 1$. In case $k = N + 1$, we have $\lim_{y \searrow d_N} \Phi'(y) < 0$ due to the minimality of k . Hence,

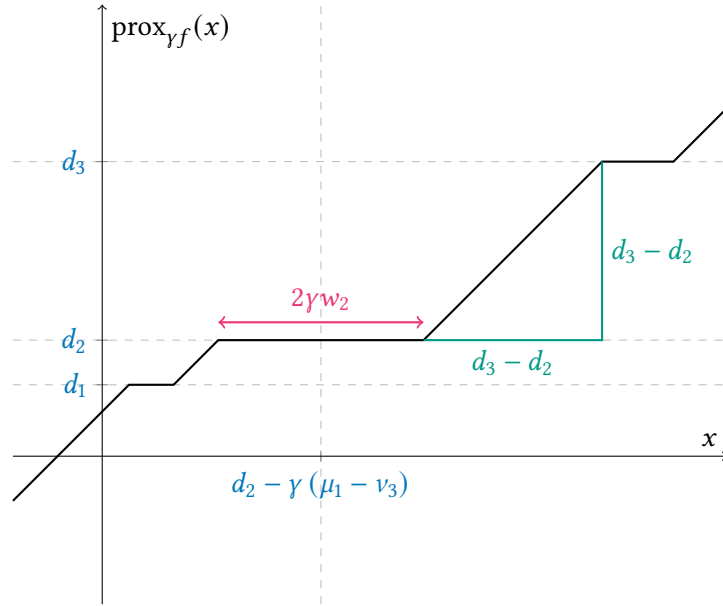
$$d_N < y^* = x - \gamma(\mu_N - \nu_{N+1}) < d_{N+1} = \infty.$$

A similar reasoning applies in the case $k = 1$. □

We provide an efficient and vectorized PYTHON implementation of [Algorithm 1](#) in [Baumgärtner et al., 2023](#). It allows the simultaneous evaluation of (1.3) for multiple values of x , provided that each instance of (1.3) has the same number N of data points. The weights w_i and data points d_i as well as the prox parameter γ may vary between instances. The discussion so far assumed positive weights for simplicity, but the case $w_i = 0$ is a simple extension and it is allowed in our implementation. This is convenient in order to simultaneously solve problem instances which differ with respect to the number of data points N . In this case, we can easily pad all instances to the same number of data points using zero weights. In addition, data points are allowed to be duplicate, i. e., we only require $d_1 \leq d_2 \leq \dots \leq d_N \in \mathbb{R}$, $N \geq 1$. Notice that since the data points are assumed to be sorted, finding the index in [Line 1](#) is of complexity $\log N$.

3 STRUCTURE OF $\text{prox}_{\gamma f}$

In this section, we briefly discuss the structure of the map $x \mapsto \text{prox}_{\gamma f}(x)$. Since it generalizes the soft-thresholding operation (1.5), it is not surprising that we obtain a graph which features a staircase pattern. An illustrative plot for certain choices of weights w_i , data points d_i , and prox parameter $\gamma > 0$ is shown in [Figure 3.1](#). Each of the N distinct data points provides one plateau in the graph.

Figure 3.1: Example of the proximal map $\text{prox}_{\gamma f}$ in case $N = 3$.

Two alternating regimes occur for $y^* = \text{prox}_{\gamma f}(x)$, as x ranges over \mathbb{R} . First, when $y^* \in \text{int } I_k$ holds, then (2.9) implies that y^* is an affine function of x with slope 1. This is the case for x whose associated index k is constant, i. e.,

$$x \in \gamma(\mu_k - v_{k+1}) + [d_k, d_{k+1}].$$

As x increases beyond the upper bound of the interval above, y^* enters a constant regime which applies to

$$x \in \gamma(\mu_{k-1} - v_{k+1}) + d_k + [-\gamma w_k, \gamma w_k].$$

Notice that the case $N = 1$ reduces to the soft-thresholding map (1.5) with only one plateau.

4 APPLICATION TO IMAGE DENOISING

In this section, we present the application of [Algorithm 1](#) to a classical (ROF) total-variation image denoising problem going back to [Rudin, Osher, Fatemi, 1992](#). Given noisy image data $f_{i,j}$ of size $D_1 \times D_2$, we seek an image $u_{i,j}$ of the same dimension which solves

$$\begin{aligned} \text{Minimize } \mathcal{H}(u) := & \frac{1}{2} \sum_{i=1}^{D_1} \sum_{j=1}^{D_2} (u_{i,j} - f_{i,j})^2 \\ & + \beta \sum_{i=1}^{D_1-1} \sum_{j=1}^{D_2} |u_{i+1,j} - u_{i,j}| + \beta \sum_{i=1}^{D_1} \sum_{j=1}^{D_2-1} |u_{i,j+1} - u_{i,j}|, \quad u \in \mathbb{R}^{D_1 \times D_2}. \end{aligned} \quad (4.1)$$

Well-known solution approaches to (4.1) include the primal-dual hybrid gradient method [Chambolle, Pock, 2011](#) and the split Bregman iteration [Goldstein, Osher, 2009](#). The latter requires the solution of a Laplacian problem for $u_{i,j}$ in each iteration. A simpler approach, considered in [Li, Osher, 2009](#), is to

partition the unknowns in (4.1) into two disjoint subsets, according to a checkerboard pattern. In this case, problem (4.1) with only one subset of unknowns decouples into independent problems, each of which is of type (1.3) with weights $w_i = 1$ and $\gamma = \beta$ and can be solved efficiently and in parallel using Algorithm 1. We give further implementation details below.

Alternating over both subsets of unknowns, one obtains a block-coordinate descent method as proposed in Li, Osher, 2009, Sec. 3. Unfortunately, such a method does not necessarily converge towards the global minimizer for non-smooth objectives; see for instance Friedman et al., 2007, Sec. 2. Therefore, Li, Osher, 2009 proposed to restart the block-coordinate descent algorithm using a random perturbation of the final iterate upon stagnation.

We depart from this restarting strategy in the following way. Upon stagnation of the block-coordinate descent method, we evaluate the steepest descent direction by orthogonally projecting (w.r.t. the Euclidean norm $\|\cdot\|$) the zero vector onto the subdifferential of the objective \mathcal{H} from (4.1):

$$d = -\operatorname{proj}_{\partial\mathcal{H}(u)}(\mathbf{0}) = -\arg\min_{s \in \partial\mathcal{H}(u)} \|s\|^2. \quad (4.2)$$

Due to the structure of the subdifferential of the absolute value function $|\cdot|$, this amounts to solving a quadratic optimization problem with $D_1 D_2$ unknowns and sparse linear equality as well as bound constraints, which describe the condition $s \in \partial\mathcal{H}(u)$. We employ the QP solver OSQP (Stellato et al., 2020, <https://github.com/osqp/osqp>) for the purpose of solving (4.2).

The steepest descent direction (4.2) is used in the following way in Algorithm 2. First, it serves as a perturbation direction upon stagnation, in contrast to the random perturbation proposed in Li, Osher, 2009; see Line 10. Second, the norm $\|d\|$ can serve as a stopping criterion; see Line 14.

Algorithm 2 Checkerboard scheme to approximately solve (4.1).

Input: tolerances $\text{TOL}_{\text{inner}}$, $\text{TOL}_{\text{outer}}$

Output: u^k , an approximate solution of (4.1)

```

1:  $k := 0$ 
2: repeat
3:   repeat
4:      $u_w^{k+1} := \arg\min_{u_w} \mathcal{H}(u_b^k + u_w)$  using Algorithm 1
5:      $u_b^{k+1} := \arg\min_{u_b} \mathcal{H}(u_b + u_w^{k+1})$  using Algorithm 1
6:     Set  $k := k + 1$ 
7:   until  $\|u^k - u^{k-1}\| \leq \text{TOL}_{\text{inner}}$ 
8:    $d := -\operatorname{proj}_{\partial\mathcal{H}(u^k)}(\mathbf{0})$ 
9:   if  $\|d\| > \text{TOL}_{\text{outer}}$  then
10:    Choose  $\alpha > 0$  with  $\mathcal{H}(u^k + \alpha d) < \mathcal{H}(u^k)$ 
11:    Set  $u^{k+1} := u^k + \alpha d$ 
12:    Set  $k := k + 1$ 
13:   end if
14: until  $\|d\| \leq \text{TOL}_{\text{outer}}$ 

```

In Lines 4 and 5, we use subvector indexing. That is, u_w refers to the subvector of u with “white”

subroutine	number of calls	total time	time per call
Algorithm 1 (32 768 solves of (1.3) in parallel)	74	10.7 s	0.14 s
solution of QP (Line 8) using OSQP	5	11.7 s	2.34 s

Table 4.1: Timing results.

indices copied and “black” indices zeroed. The roles are reversed for u_b . Consequently, $u = u_b + u_w$ holds. Subvector indexing can be conveniently done in PYTHON using logical indexing.

Notice that [Lines 4](#) and [5](#) require the evaluation of a function of the (1.3) for many arguments in parallel, where we benefit from our vectorized implementation of [Algorithm 1](#). All norms in [Theorem 2.1](#) are Frobenius norms for matrices. [Line 10](#) is implemented using a backtracking strategy starting with initial step size $\alpha = 0.5$, which is then halved until the condition $\mathcal{H}(u^k + \alpha d) < \mathcal{H}(u^k)$ is met.

We wish to emphasize that we do not propose [Algorithm 2](#) as a novel solver for image denoising problems. We rather consider it here as a source of problems of type (1.3), which can be solved efficiently by our proposed [Algorithm 1](#). In practice, [Algorithm 2](#) can also be used effectively as a preliminary solver stage for (4.1), before one switches to, e. g., the split Bregman or Chambolle-Pock iteration.

For verification purposes, we show the outcome of [Algorithm 2](#). As a test case, we choose the well-known cameraman image of size $D_1 = D_2 = 256$. We add zero-mean Gaussian noise with standard deviation $\sigma = 50$ independently pixel by pixel. We then truncate the values to the range $[0, 255]$ to obtain the noisy image shown in [Figure 4.1a](#). We apply [Algorithm 2](#) to the image denoising problem (4.1) with parameter $\beta = 10$. The inner tolerance is set to $\text{TOL}_{\text{inner}} = 10^{-4}$. We observe that even for a coarse outer tolerance of $\text{TOL}_{\text{outer}} = 300$, a good reconstruction is obtained; see [Figure 4.1b](#). This tolerance is reached after $k = 42$ iterations, of which 37 are iterations of the loop in [Line 4–Line 6](#) and 5 are executions of [Line 8–Line 13](#). In particular, the subdifferential projection step in [Line 8](#), which amounts to solving a quadratic optimization problem, is carried out 5 times. For comparison, we include an “exact” solution of (4.1) obtained by a split Bregman iteration with very tight tolerances in [Figure 4.1](#).

Each call to [Algorithm 1](#) ([Lines 4](#) and [5](#) in [Algorithm 2](#)) evaluates the proximity operator (1.3) in parallel for half the number of pixels, i. e., $2^{15} = 32\,768$ instances. Using padding with zero weights for instances of (1.3) pertaining to points on the boundary, all instances have $N = 4$ data points d_i (the current values for all neighbors north, south, east and west) and weights $w_i \in \{0, 1\}$. Timing results are reported in [Table 4.1](#). They were obtained on a laptop with an 8-core Intel Core i5 CPU with 1.6 GHz and 16 GiB RAM, running Ubuntu 22.04 and PYTHON 3.10.

5 APPLICATION TO A DEFLECTION ENERGY MINIMIZATION PROBLEM

In this section, we consider the minimization of the non-smooth energy \mathcal{J} of a deflected membrane. We apply an ADMM (alternating direction method of multipliers) scheme which requires the parallel



(a) Noisy cameraman image.



(b) Approximate solution obtained with Algorithm 2.



(c) Exact solution of (4.1) obtained by a split Bregman iteration.

Figure 4.1: Numerical results to obtain timings for Algorithm 1.

evaluation of the proximal map Algorithm 1 in each inner loop of the scheme.

Consider a bounded domain $\Omega \subset \mathbb{R}^2$ occupied by a thin membrane. In our model, the energy of this membrane is given in terms of its unknown deflection (displacement) function $z: \Omega \rightarrow \mathbb{R}$ and it takes the following form:

$$\mathcal{J}(z) = \frac{1}{2} \int_{\Omega} c |\nabla z|^2 dx - \int_{\Omega} f z dx + \sum_{i=1}^L w_i \int_{\Omega} \max\{z - d_i, 0\} dx + \frac{1}{2} \int_{\Gamma} \alpha z^2 ds. \quad (5.1)$$

The first term describes the potential energy of the membrane, where $c \in \mathbb{R}$ is the stiffness constant. The second term accounts for an external area force density f , which we assume to be a non-negative function on Ω . Consequently, the deflection will be non-negative as well. The specialty of our model is the third term, which can be interpreted as follows. The non-negative constants d_1, \dots, d_L serve as thresholds.¹ Once the deflection z at a point in Ω exceeds any of these thresholds d_i , an additional downward force of size $w_i > 0$ times the excess deflection activates. Finally, the fourth term models an additional potential energy due to springs along the boundary Γ of the domain with stiffness constant α . A related problem has been studied in [Bostan, Han, Reddy, 2005](#) with an emphasis on a posteriori error analysis and adaptive solution.

Notice that the minimization of the convex, non-smooth energy \mathcal{J} among all displacements $z \in H^1(\Omega)$ corresponds to the weak form of a partial differential equation (PDE), or rather a variational inequality. In fact, the necessary and sufficient optimality conditions for the minimization of (5.1) amount to

$$\begin{aligned} c \int_{\Omega} \nabla z \cdot \nabla \delta z dx - \int_{\Omega} f \delta z dx + \sum_{i=1}^L w_i \int_{\Omega} \chi_{\{x \in \Omega \mid z(x) > d_i\}} \delta z dx \\ + \sum_{i=1}^L w_i \int_{\Omega} \chi_{\{x \in \Omega \mid z(x) = d_i\}} \max\{\delta z, 0\} dx + \int_{\Gamma} \alpha z \delta z ds \geq 0 \quad \text{for all } \delta z \in H^1(\Omega). \end{aligned} \quad (5.2)$$

Here, $\chi_A: \Omega \rightarrow \mathbb{R}$ is the characteristic function of the set A with values in $\{0, 1\}$. Provided that the set $\{x \in \Omega \mid z(x) = d_i\}$ is of Lebesgue measure zero, the variational inequality (5.2) becomes an equation,

¹We could also allow d_1, \dots, d_L to be non-negative functions on Ω , with minor modifications in what follows.

whose strong form—using integration by parts—can be seen to be

$$\begin{aligned} -c \Delta z + \sum_{i=1}^L w_i \chi_{\{x \in \Omega \mid z(x) > d_i\}} &= f \quad \text{in } \Omega, \\ c \frac{\partial z}{\partial n} &= \alpha z \quad \text{on } \Gamma. \end{aligned}$$

From here we also learn that the boundary term in the energy (5.1) leads to boundary conditions of Robin type.

We employ a standard Galerkin approach to numerically discretize the energy (5.1). To this end, we replace the displacement space $H^1(\Omega)$ by some finite dimensional subspace of piecewise linear, globally continuous finite element functions defined over a triangulation of Ω . Denoting the associated nodal basis by $\{\varphi_i\}$, we define the stiffness matrix

$$K_{ij} = \int_{\Omega} c \nabla \varphi_i \cdot \nabla \varphi_j \, dx + \int_{\Gamma} \alpha \varphi_i \varphi_j \, ds$$

as well as the lumped mass matrix

$$M_{ii} = \int_{\Omega} \varphi_i \, dx$$

with $M_{ij} = 0$ when $i \neq j$. The reason for using mass lumping to approximate all area integrals in (5.1) which do not involve derivatives is to translate the pointwise maximum operator into a coefficientwise one. This technique is crucial for an efficient numerical realization and has been used before, e. g., in Wachsmuth, Wachsmuth, 2011; Casas, Herzog, Wachsmuth, 2012.

We continue to use z to denote the nodal values of the finite element discretization of the deflection and thus obtain the discrete energy

$$\mathcal{J}_h(z) = \frac{1}{2} z^T K z - f^T M z + \sum_{i=1}^L w_i \mathbf{1}^T M \max\{z - d_i, 0\}. \quad (5.3)$$

Here, $\mathbf{1}$ denotes the vector of all ones and the max operation is understood coefficientwise.

The minimization of the convex but non-smooth energy (5.3) is not straightforward. Our method of choice here is an ADMM scheme, which moves the non-smooth terms into a separate subproblem, which can then be efficiently solved using Algorithm 1. We refer the reader to Boyd et al., 2010 and the references therein for an overview on ADMM.

In order to obtain a subproblem of type (1.3), we use the identity $2 \max\{a, b\} = a + b + |a - b|$ and arrive at

$$\mathcal{J}_h(z) = \frac{1}{2} z^T K z - \tilde{f}^T M z + \frac{1}{2} \sum_{i=1}^L w_i \mathbf{1}^T M |z - d_i| + C \quad (5.4)$$

where $C := \sum_{i=1}^L w_i d_i \mathbf{1}^T M \mathbf{1}$ is a constant and $\tilde{f} := f - \frac{1}{2} \sum_{i=1}^L w_i \mathbf{1}$ is a modification of the force vector. Moreover, the absolute value $|\cdot|$ is understood coefficientwise. Dropping the constant C , introducing

a second variable y , the constraint $z = y$ and associated (scaled) Lagrange multiplier μ gives rise to the augmented Lagrangian

$$\mathcal{L}_\rho(z, y, \mu) = \frac{1}{2}z^\top Kz - \tilde{f}^\top Mz + \frac{1}{2} \sum_{i=1}^L w_i \mathbf{1}^\top M |y - d_i \mathbf{1}| + \frac{\rho}{2} \|z - y + \mu\|_M^2, \quad (5.5)$$

where $\|\cdot\|_M^2$ is the squared norm induced by the positive diagonal matrix M .

An ADMM computes iterates $z^{(k)}$, $y^{(k)}$, $\mu^{(k)}$ according to the following update scheme

$$z^{(k+1)} := \arg \min_z \mathcal{L}_\rho(z, y^{(k)}, \mu^{(k)}), \quad (5.6a)$$

$$y^{(k+1)} := \arg \min_y \mathcal{L}_\rho(z^{(k+1)}, y, \mu^{(k)}), \quad (5.6b)$$

$$\mu^{(k+1)} := \mu^{(k)} + z^{(k+1)} - y^{(k+1)}. \quad (5.6c)$$

For the problem at hand, (5.6a) amounts to the solution of the discretized Poisson-like problem

$$Kz + \rho Mz = M(\tilde{f} + \rho(y^{(k)} - \mu^{(k)})).$$

The y -update (5.6b) on the other hand can be cast as the problem

$$\text{Minimize } \frac{1}{2} \sum_{i=1}^L w_i \mathbf{1}^\top M |y - d_i \mathbf{1}| + \frac{\rho}{2} \|z^{(k+1)} - y + \mu^{(k)}\|_M^2 \quad \text{w.r.t. } y. \quad (5.7)$$

Owing to the diagonal structure of the mass matrix, this problem fully decouples, the mass matrix cancels, and we obtain

$$\text{Minimize } \frac{1}{2} \sum_{i=1}^L w_i |y_j - d_i| + \frac{\rho}{2} (z_i^{(k+1)} - y_j + \mu_i^{(k)})^2 \quad \text{w.r.t. } y_j \quad (5.8)$$

for each component y_j of y . This problem fits into the pattern of (1.3), and thus can be solved efficiently and simultaneously for all components y_j by [Algorithm 1](#).

In order to validate the method, we consider two simple, convex domains

$$\Omega_1 := (0, 1)^2, \quad \Omega_2 := (0, 1.1)^2 \setminus (0.6, 1.1)^2.$$

We use meshes with 2521 vertices for Ω_1 and 2637 vertices for Ω_2 . We choose the stiffness constant c , force density f , boundary stiffness constant α , additional downward forces w_i and threshold deflections d_i to be constant over the domains in each case, as

$$c \equiv 1, \quad f \equiv 0.5, \quad \alpha \equiv 10, \quad d_i \equiv 0.01 \cdot i, \quad w_i \equiv 0.02, \quad i = 1, \dots, 4. \quad (5.9)$$

We apply the ADMM scheme (5.6). The iterations are terminated as soon as the stopping criterion

$$\max\{\|z^{(k+1)} - z^{(k)}\|_M, \|y^{(k+1)} - y^{(k)}\|_M, \|\mu^{(k+1)} - \mu^{(k)}\|_M\} \leq \text{TOL} := 10^{-20} \quad (5.10)$$

is satisfied, where we recall that $\|\cdot\|_M$ denotes the norm induced by the lumped mass matrix M . With this setup and $\rho = 100$, the ADMM algorithm required 186 iterations for the problem on Ω_1 and 278 iterations in case of Ω_2 . The resulting solutions z are shown in [Figure 5.1](#).



Figure 5.1: Resulting deflections z which minimize the discrete energy functional \mathcal{J}_h defined in (5.3) over two different domains, with data given in (5.9). Deflections were computed with the ADMM scheme (5.6) and stopping criterion (5.10). The subdomains are colored according to the number of active terms ($z \geq d_i$) in (5.3).

REFERENCES

- Baumgärtner, L.; R. Herzog; S. Schmidt; M. Weiß (2023). *The proximal map of the weighted mean absolute error*. DOI: [10.5281/zenodo.7620815](https://doi.org/10.5281/zenodo.7620815).
- Bauschke, H. H.; P. L. Combettes (2011). *Convex Analysis and Monotone Operator Theory in Hilbert Spaces*. CMS Books in Mathematics/Ouvrages de Mathématiques de la SMC. Springer, New York. DOI: [10.1007/978-1-4419-9467-7](https://doi.org/10.1007/978-1-4419-9467-7).
- Bostan, V.; W. Han; B. D. Reddy (2005). “A posteriori error estimation and adaptive solution of elliptic variational inequalities of the second kind”. *Applied Numerical Mathematics. An IMACS Journal* 52.1, pp. 13–38. DOI: [10.1016/j.apnum.2004.06.012](https://doi.org/10.1016/j.apnum.2004.06.012).
- Boyd, S.; N. Parikh; E. Chu; B. Peleato; J. Eckstein (2010). “Distributed optimization and statistical learning via the alternating direction method of multipliers”. *Foundations and Trends in Machine Learning* 3.1, pp. 1–122. DOI: [10.1561/2200000016](https://doi.org/10.1561/2200000016).
- Casas, E.; R. Herzog; G. Wachsmuth (2012). “Approximation of sparse controls in semilinear equations by piecewise linear functions”. *Numerische Mathematik* 122.4, pp. 645–669. DOI: [10.1007/s00211-012-0475-7](https://doi.org/10.1007/s00211-012-0475-7).
- Chambolle, A.; T. Pock (2011). “A first-order primal-dual algorithm for convex problems with applications to imaging”. *Journal of Mathematical Imaging and Vision* 40.1, pp. 120–145. DOI: [10.1007/s10851-010-0251-1](https://doi.org/10.1007/s10851-010-0251-1).
- Chen, S. S.; D. L. Donoho; M. A. Saunders (1998). “Atomic decomposition by basis pursuit”. *SIAM Journal on Scientific Computing* 20.1, pp. 33–61. DOI: [10.1137/s1064827596304010](https://doi.org/10.1137/s1064827596304010).
- Combettes, P. L.; J.-C. Pesquet (2011). “Proximal splitting methods in signal processing”. *Fixed-Point Algorithms for Inverse Problems in Science and Engineering*. Vol. 49. Springer Optimization and Its Applications. Springer, New York, pp. 185–212. DOI: [10.1007/978-1-4419-9569-8_10](https://doi.org/10.1007/978-1-4419-9569-8_10).
- Daubechies, I.; M. Defrise; C. De Mol (2004). “An iterative thresholding algorithm for linear inverse problems with a sparsity constraint”. *Communications on Pure and Applied Mathematics* 57.11, pp. 1413–1457. DOI: [10.1002/cpa.20042](https://doi.org/10.1002/cpa.20042).
- Friedman, J.; T. Hastie; H. Höfling; R. Tibshirani (2007). “Pathwise coordinate optimization”. *The Annals of Applied Statistics* 1.2, pp. 302–332. DOI: [10.1214/07-AOAS131](https://doi.org/10.1214/07-AOAS131).
- Goldstein, T.; S. Osher (2009). “The split Bregman method for L_1 -regularized problems”. *SIAM Journal on Imaging Sciences* 2.2, pp. 323–343. DOI: [10.1137/080725891](https://doi.org/10.1137/080725891).

- Li, Y.; S. Osher (2009). “A new median formula with applications to PDE based denoising”. *Communications in Mathematical Sciences* 7.3, pp. 741–753. DOI: [10.4310/cms.2009.v7.n3.a11](https://doi.org/10.4310/cms.2009.v7.n3.a11).
- Parikh, N.; S. Boyd (2014). “Proximal algorithms”. *Foundations and Trends in Optimization* 1.3, pp. 127–239. DOI: [10.1561/2400000003](https://doi.org/10.1561/2400000003).
- Rudin, L. I.; S. Osher; E. Fatemi (1992). “Nonlinear total variation based noise removal algorithms”. *Physica D* 60.1–4, pp. 259–268. DOI: [10.1016/0167-2789\(92\)90242-F](https://doi.org/10.1016/0167-2789(92)90242-F).
- Stellato, B.; G. Banjac; P. Goulart; A. Bemporad; S. Boyd (2020). “OSQP: an operator splitting solver for quadratic programs”. *Mathematical Programming Computation* 12.4, pp. 637–672. DOI: [10.1007/s12532-020-00179-2](https://doi.org/10.1007/s12532-020-00179-2).
- Tibshirani, R. (1996). “Regression shrinkage and selection via the Lasso”. *Journal of the Royal Statistical Society. Series B. Methodological* 58.1, pp. 267–288. DOI: [10.1111/j.2517-6161.1996.tb02080.x](https://doi.org/10.1111/j.2517-6161.1996.tb02080.x).
- Wachsmuth, G.; D. Wachsmuth (2011). “Convergence and regularization results for optimal control problems with sparsity functional”. *ESAIM: Control, Optimisation and Calculus of Variations* 17.3, pp. 858–886. DOI: [10.1051/cocv/2010027](https://doi.org/10.1051/cocv/2010027).